

The Advantage of an Integrated RTK-GPS System in Monitoring Structural Deformation

Xaiojing Li

Schools of Electrical Engineering & Telecommunications, School of Surveying & Spatial Information Systems, The University of New South Wales, Sydney NSW 2052, Australia
Email: xj.li@unsw.edu.au; Tel: 61-2-9385 5534, Fax: 61-2-9385 5388

Received: 15 Nov 2004 / Accepted: 3 Feb 2005

Abstract. Monitoring structural response induced by severe loadings such as typhoon is an efficient way to mitigate or prevent damage. Because the measured signal can be used to activate an alarm system to evacuate people from an endangered building, or to drive a control system to suppress typhoon excited vibrations so as to protect the integrity of the structure. A 108m tall tower in Tokyo has been monitored by an integrated system combining RTK-GPS and accelerometers. Data collected by the multi-sensor system have been analysed and compared to the original finite element modeling (FEM) result for structural deformation monitoring studies. Especially, the short time Fast Fourier Transform (FFT) analysis results have shown that the time-frequency relation does give us almost instantaneous frequency response during a typhoon event. In this paper the feasibility of integrating advanced sensing technologies such as RTK-GPS with traditional accelerometer sensors, for structural vibration response and deformation monitoring under severe loading conditions, is discussed. The redundancy within the integrated system has shown robust quality assurance.

Key words: vibration, displacement, deformation, integrity, structural response

1. Introduction

Civil engineering structures are typically designed based on the principles of material and structural mechanics. Finite element model (FEM) analysis and wind tunnel tests of scaled models are often carried out to assist structural design (see, e.g., Penman et al, 1999). However, loading conditions in the real world are always

much more complicated than can be imagined, and hence key man-made structures must be monitored to ensure that they maintain integrity of design, construction and operation.

In general, until recently, monitoring the dynamic response of civil structures for the purpose of assessment of damage has relied on measurements from accelerometer sensors deployed on the structure. Studies conducted on such data records have been useful in assessing structural design procedures, improving building codes and correlating the response of the structure with the damage caused. However, a double integration process is required to arrive at the relative displacements, and there is no way to recover the static or quasi-static displacement from the acceleration. Also it is difficult to overcome drift natural to the accelerometer. Therefore, it has been proposed to integrate an accelerometer sensor with GPS and other sensors in order to best utilize the advantageous properties of each.

In contrast to accelerometers, GPS can measure directly the position coordinates (Parkinson & Spilker, 1996), hence providing an opportunity to monitor, in real-time and full scale, the dynamic characteristics of the structure to which the GPS antennas are attached. In order to achieve cm-level accuracy, the standard mode of precise differential GPS positioning locates one reference receiver at a base station whose three dimensional coordinates are known, so that the second receiver's coordinates are determined relative to this reference receiver. Preliminary studies have proven the technical feasibility of using GPS to monitor dynamic structural deformation due to winds, traffic, earthquakes and similar loading events in, e.g., the UK (Ashkenazi and Roberts, 1997), USA (Kilpatrick et al, 2003), Singapore (Brownjohn et al, 1998) and Japan (Tamura et al, 2002). Although GPS offers real-time solutions, it has its own limitations. For example, GPS can only sample at a rate of up to 20Hz (Trimble, 2003), although higher rates may be possible in the future.

The paper is organized as follows. The second part presents an analysis of data collected using GPS, accelerometer and anemometer sensors while monitoring the responses of a 108m tall steel tower during Typhoon No. 21 on the first of October 2002. The third part discusses the necessity of integration of GPS and accelerometer sensors; and finally the paper concludes with a summary of the research findings.

2. Deformations Monitored by RTK-GPS and Accelerometer

2.1 The field monitoring system

As part of the collaborative research between the Tokyo Polytechnic University and the UNSW, a combined RTK-GPS and accelerometer system has been deployed on a 108m steel tower in Tokyo owned by the Japan Urban Development Corporation, in order to monitor the tower’s deformation on a continuous basis. At the top of the tower, a GPS antenna together with accelerometers and an anemometer were installed. Another GPS antenna was setup on the top of a 16m high rigid building, as a reference point 110m away from the tower. In addition, strain gauges were set in the foundation of the tower to measure member stresses. Figure 1 illustrates the experimental setup. Note the local/monitoring coordinate system has been established so that X is East, Y is North and Z is pointing to the zenith.

The RTK-GPS and accelerometer data were recorded at 10Hz and 20Hz sampling rates respectively. And the data was collected from 19:00 to 21:00 Japan Standard Time (JST) during Typhoon No. 21 on 1 October 2002 (Tamura et al., 2002). Because the weather was cloudy and rainy the solar heating effect on the steel tower will be ignored in the analysis of later sections.

It is well known that light, flexible buildings are more favorable for resisting seismic force, while heavy, stiff buildings are more favorable for resisting wind force. Tall buildings in Japan have to satisfy these two opposite design criteria, and this is one of the most difficult design issues for tall buildings in Japan. The focus in this paper will be only on the effects of typhoon on the 108 m tower.

2.2 Typhoon data set

The overall plots of time series of the RTK-GPS measured displacements in X, Y and Z directions are shown in Figure 2. Measurements from the

accelerometers (X and Y directions only) are given in Figure 4. From the least-squares polynomial fitting (blue lines) in Figure 2 the maximum displacements in the X and Y directions are around 5.8cm and -4.5cm respectively, indicating significant static and quasi-static movements. However in the Z direction the signal seems to bounce between 2cm and -2cm. This confirms the less accurate characteristics of the vertical measurement by using GPS. Figure 3 are the recorded wind speed and direction time series. The higher speed corresponds to larger displacement and stronger acceleration. The changes of the wind direction agreed with the signs of displacements in X and Y direction measured by RTK-GPS. For example, at 20:00 the wind was NW (Figure 9). Therefore, the displacements on X and Y directions should be positive and negative respectively and this is exactly what the GPS has recorded (Figure 2).

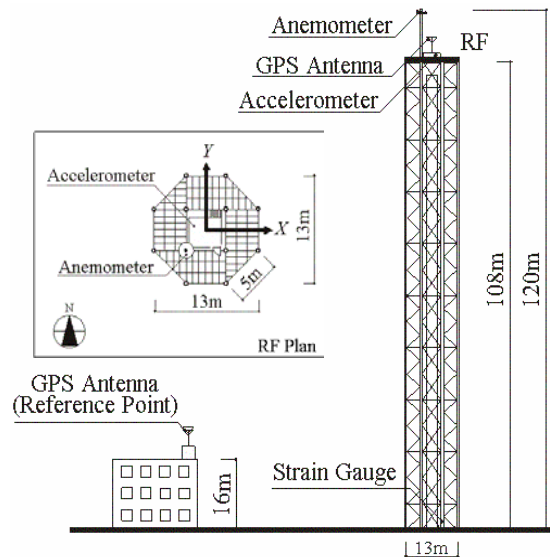


Figure 1 The 108m steel tower used for deformation monitoring study.

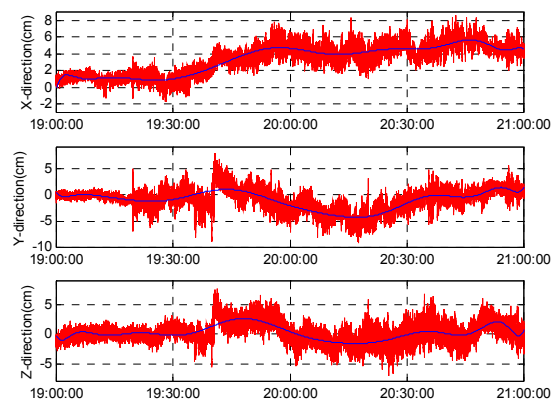


Figure 2 Displacement measured by RTK-GPS.

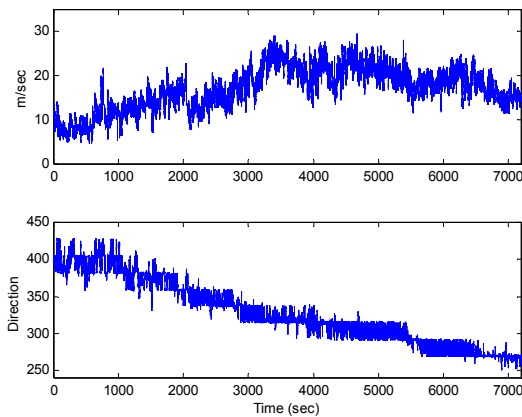


Figure 3 Wind speed and direction time series.

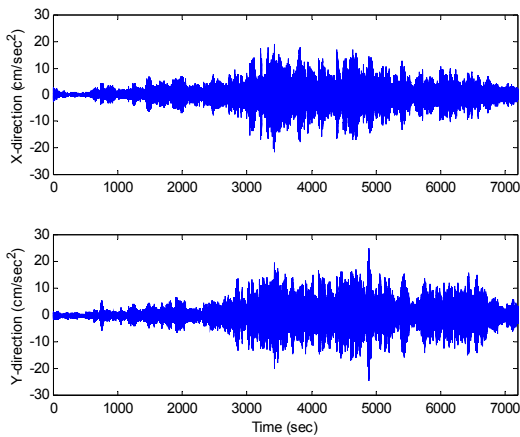


Figure 4 Acceleration measured by accelerometer.

2.3 Signals obtained from the typhoon data set

According to a previous study on the basic characteristics and applicability of RTK-GPS (Tamura et al, 2002), GPS results seem to follow closely the actual displacement under conditions when the vibration frequency is lower than 2Hz, and the vibration amplitude is larger than 2cm. Consequently it is possible to assess the accuracy of recorded data by analysing the spectrum of the wind-induced vibration of the tower. Using the FFT and zooming in the RTK-GPS spectrum, it is obvious that there is a 0.57Hz component in the Y direction (blue peak in Figure 5). However, in the X direction (red) there are two peaks at 0.54Hz and 0.61Hz. In the 0–0.20Hz range, the static and quasi-static responses can be clearly distinguished by comparing with the wind speed fluctuation spectrum Figure 6. And the noises such as multipath are contributing to all three directions coupled in the 0.05-0.2Hz range.

Figure 7 is a zoom-in of the accelerometer spectrum. It appears to be very clean at the lower frequency end (0 to 0.20Hz). It is obvious also that there is a 0.57Hz component in the Y direction (green peak). However, in the X direction (blue peaks) there are two peaks at 0.54Hz and 0.61Hz by further zooming in, which are identical to what RTK-GPS has picked up. In addition, there are less significant peaks around 1.86Hz and 2.16Hz for both the X and Y directions, while at 1.86Hz the X direction is much stronger than the Y. In the meantime, the overall FFT spectrum gives a peak at 4.56Hz as well (Figure 23).

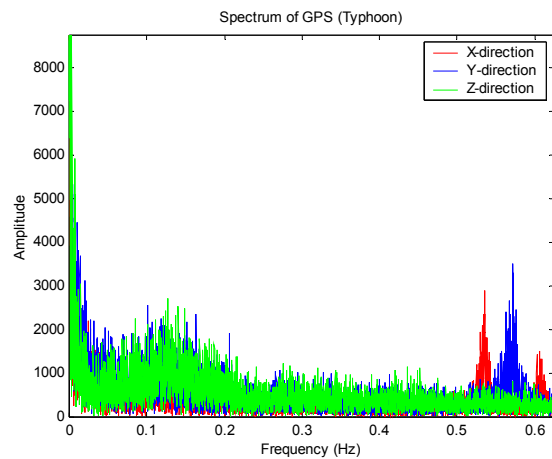


Figure 5 Zoom-in of the FFT spectrum of RTK-GPS.

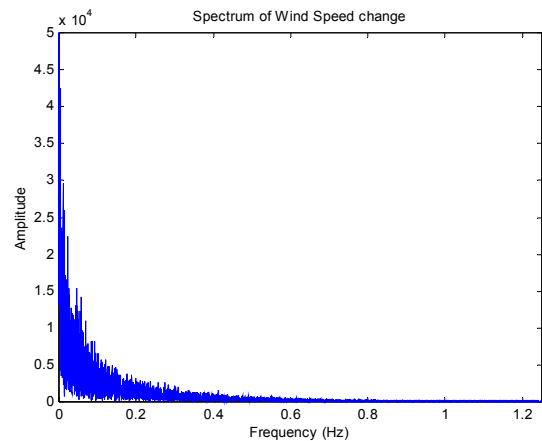


Figure 6 The wind speed fluctuation spectrum.

According to the anemometer recordings, the wind direction was mostly North and North-West during the two hour experiment. Figure 8 gives the mean direction every 51.2 seconds. North corresponds to the Y-direction of the monitoring system. Hence, it is useful to focus on the Y direction (blue in Figure 5).

It is clear that the spectrums for both the accelerometer and RTK-GPS have the dominant frequency of 0.57Hz, indicating that it is the lowest natural frequency of the steel tower. This result agrees with Tamura et al (2002),

using the power spectral density analysis and the random decrement (RD) technique through other typhoon event recording. FEM and frequency domain decomposition (FDD) analysis has also confirmed that 0.57Hz is the first mode natural frequency of the tower, 2.16Hz and 4.56Hz are the 2nd mode and 3rd mode respectively (Figure 9, after Yoshida et al, 2003). Although it is not clear what are the driving factors for the other peaks, there is no doubt that the GPS and accelerometer are complementary (by comparing Figures 5 and 7).

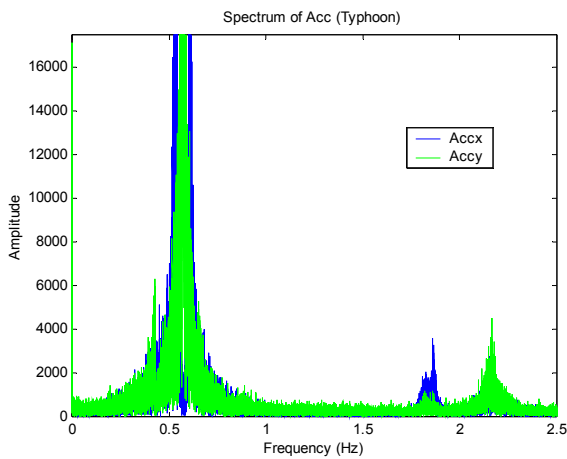


Figure 7 Zoom-in of the FFT spectrum of accelerometer.

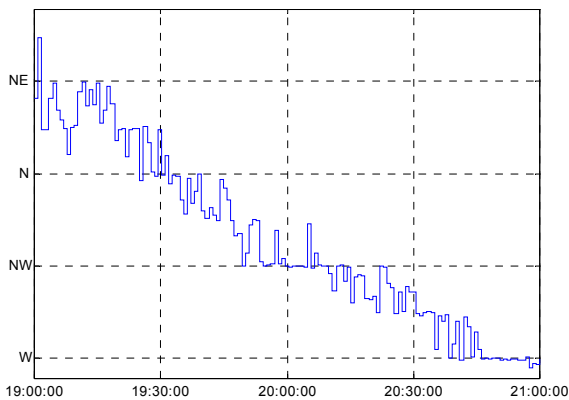


Figure 8 Wind direction change in 51.2s mean.

2.4 Wind-induced response of the tower: comparison between RTK-GPS and accelerometer

Wind-induced response of a structure generally consists of three components: a static component due to mean wind force; a quasi-static component caused by the low frequency wind force fluctuations; and a resonant component caused by the wind force fluctuation near the structure’s first mode natural frequency (Tamura, 2003).

Can the integrated GPS and accelerometer system provide all of the required information? The answer is probably “yes”. Yet no single sensor can do it alone. From the signal analysis in Section 2.3, the GPS sensor gives more information at the low frequency end while the accelerometer sensor gives more at the high frequency end. This means that both of them lose information which is very important for civil engineers. The following analysis will study this problem in more detail.

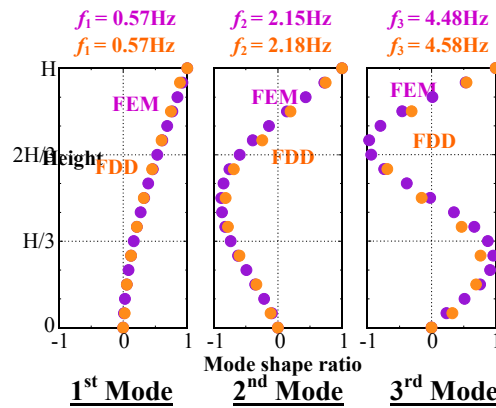


Figure 9 Modes shape obtained by FEM and FDD.

First, a double differentiation procedure is applied to a segment of RTK-GPS measured displacements data (both X and Y directions) of 100 second duration in order to convert them into acceleration. Figures 10 and 12 show the results of acceleration derived from RTK-GPS measured displacements, compared to accelerometer-measured accelerations. In the figures, the upper plots are the GPS displacements; the middle plots are the accelerations derived from the GPS measurements; and the bottom plots are the accelerometer-measured accelerations. Comparing the time series in the middle and bottom plots, it can be seen that they agree very well with each other, although the accelerometer does reveal more high frequency details, as indicated from the FFT spectrum analysis previously.

The reverse data processing is also possible. The same segments of RTK-GPS data (Figure10 and 12) are compared with the displacements derived from corresponding accelerometer measurements through a double integration process. In Figures 11 and 13, the red and blue are displacements measured by GPS and derived from accelerometer data respectively. The green and pink lines are the results of polynomial fitting. From the results shown in Figures 11 and 13, it can be seen that the vibrations (dynamic components) can be related to each other. But it is very hard to compare them quantitatively because the static and quasi-static displacements are missing from the accelerometer derived results, since there is no way to determine the integration constant.

Note that no intentional offset is used when plotting the two results.

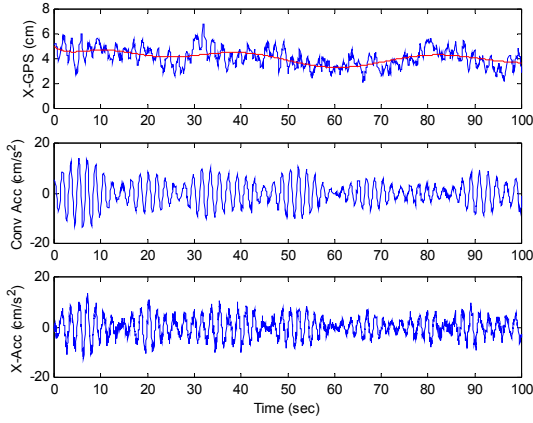


Figure 10 RTK-GPS derived and accelerometer-measured accelerations (X-direction).

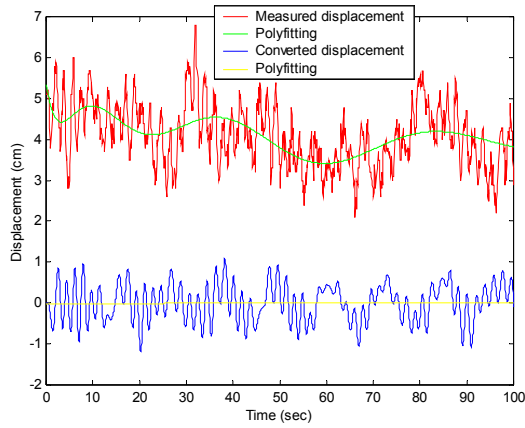


Figure 11 RTK-GPS measured and accelerometer derived displacements (X-direction).

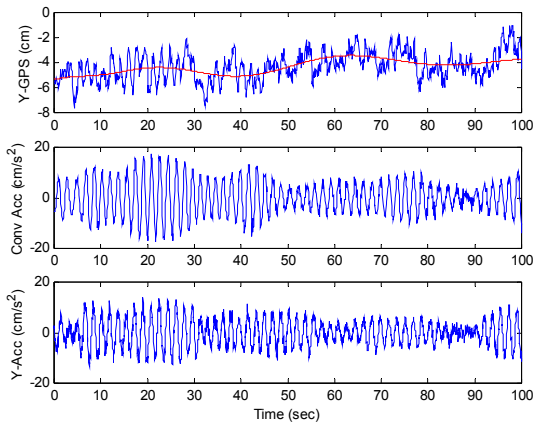


Figure 12 RTK-GPS derived and accelerometer-measured accelerations (Y-direction).

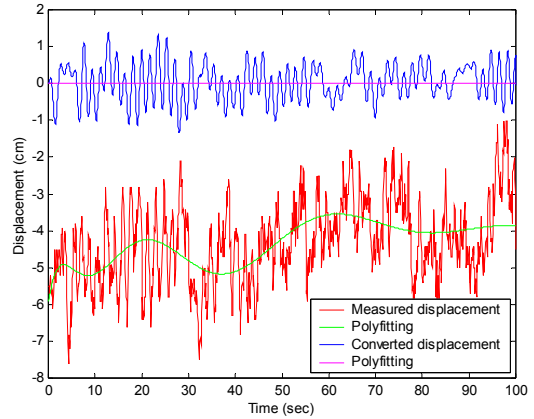


Figure 13 RTK-GPS measured and accelerometer derived displacements (Y-direction).

2.5 Time-Frequency analysis

The results of Section 2.3 are obtained by using the global FFT, whose spectrum represents the frequency composition of the WHOLE time series. It tells the relative strength (amplitude) of the frequency components, but does NOT tell when a particular frequency component occurs or takes over as the most significant frequency. It might be very useful to assess the response of or damage to the structure if it can be detected when a particular frequency component becomes dominant. A way of determining this frequency-time relationship is to apply the FFT to a short segment of the time series each time, or the so-called short time FFT analysis.

Consider the measured digital signal of $x[n]$ as a time series with respect to t . The spectrum $X[f_a]$ obtained by using Fourier transform of a discrete signal (DTFT) is a function of t , which can be derived as follows. First, Fourier transform of a discrete signal (Ambikairajah, 2003) is:

$$X[\theta] = \sum_{n=-\infty}^{\infty} x[n]e^{-jn\theta}, \quad -\pi \leq \theta \leq \pi \quad (1)$$

Where, $\theta = \omega T$ is the relative frequency, T is sampling period, ω is the frequency in radians.

Considering f_a is the frequency of the signal, and $\omega = 2\pi f_a$. The sampling frequency is determined as $f_s = \frac{1}{T}$. Therefore, θ can be given by:

$$\theta = 2\pi \frac{f_a}{f_s} \quad (2)$$

Then, the time length t of the measurements can be calculated by using the sampling period T multiple the numbers of samples n .

$$t = nT, \quad 0 \leq n \leq N \quad (3)$$

Substituting Eq. (1) with (2) and (3), Eq. (1) can be rewritten as:

$$\begin{aligned} X[f_a] &= \sum_{n=0}^N x[n] e^{-jn2\pi \frac{f_a}{f_s}} = \sum_{n=0}^N x[n] e^{-j2\pi f_a nT} \\ &= \sum_{n=0}^N x[n] e^{-j2\pi f_a t} \end{aligned} \quad (4)$$

Hence, from Eq. (4) we can see that the frequency f_a of the digital signal $x[n]$ is a function of time t . When t approaches zero, the output frequency from DTFT becomes as the instantaneous frequency. In other words, by applying DTFT on small samples of measurements, the frequency- time relationship can be established. The instantaneous frequency output can be expressed as:

$$X[f_a] = \sum_{n=N_1}^{N_2} x[n] e^{-j2\pi f_a t}, \quad \Delta n = N_2 - N_1 \ \& \ t = \Delta nT \quad (5)$$

By taking the samples Δn in power of 2, the efficient algorithm for the short time FFT analysis is obtained.

We can now use Eq. (5) to analyze the tower's frequency response with respect to time during this typhoon event. In order to represent the typical frequency which appeared in the FFT spectrum, it is important to select appropriate number of samples of measurements to be analysed each time, and only the maximum peak to be taken into account. Figures 14 and 15 are the results for GPS measurements. A total of 512 samples were processed each time. Hence the time length is 51.2s. It can be seen clearly by comparing Figure 16 that when the wind speed was over 20m/s, the tower's first mode natural frequency 0.57Hz became dominant in Y direction. The peaks of 0.61Hz and 0.54Hz appeared in X direction at different instants of time. Figure 17 is the wind speed measurement analyzed by the short time FFT, given us that the wind force fluctuation between 0.02-0.05 Hz mostly. This can be used to explain the static and quasi-static components of the wind induced response of the tower.

The time-frequency results from the accelerometer measurements are shown in Figures 18, 19, 20 and 21. Figures 18 and 19 are analyzed in window length of 128 samples. Therefore the frequency with maximum amplitude will be registered every 6.4 seconds. In Figure 18, the two frequencies of 2.16 Hz and 1.86Hz which have been picked up by using global FFT analysis in X direction appeared at different instants of time as well. It could be caused by the change of wind speed and

direction. The frequency of 0.57 Hz is the central of the appeared frequency bandwidth.

Figures 20 and 21 are processed with a window length of 256 samples. These two figures give us more clearly frequency boundary of the first mode natural vibration of the tower. Furthermore, it looks like that the tower responded with the higher mode vibration of small displacement to show that it is almost still in the weak wind, i.e. when the wind speed is lower than 10m/s.

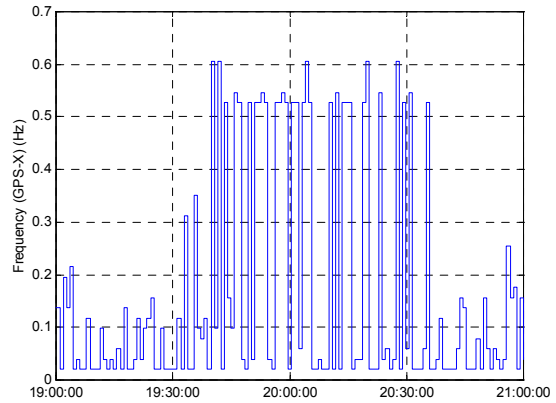


Figure 14 Time-Frequency for GPS x-dir analysis.

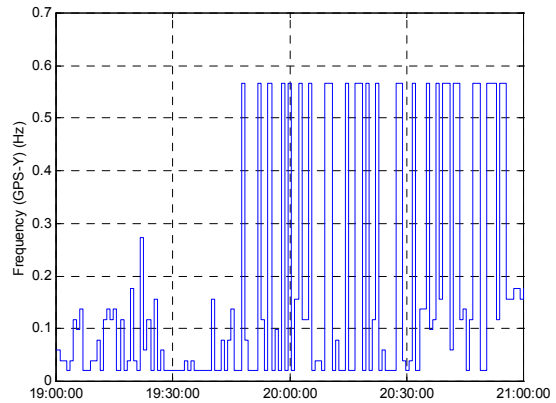


Figure 15 Time-Frequency for GPS y-dir analysis.

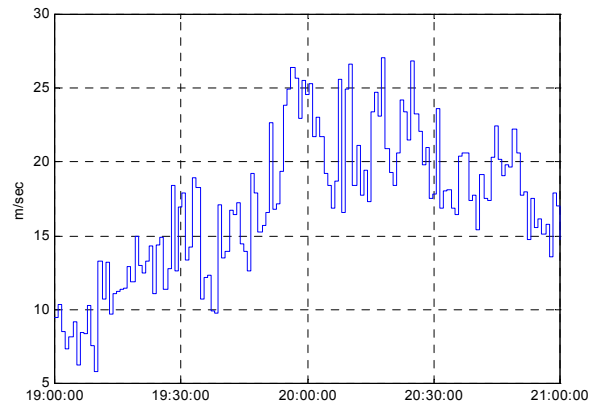


Figure 16 Mean wind speed every 51.2 seconds.

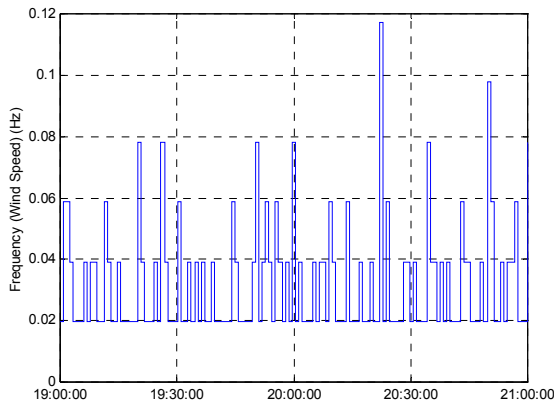


Figure 17 Time-Frequency for wind speed fluctuation.

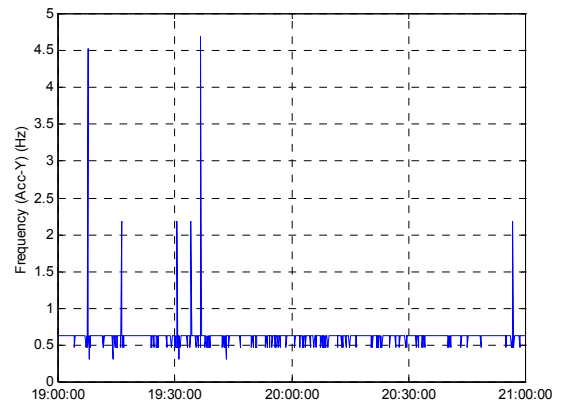


Figure 19 Time-Frequency analysis for Acc y-dir with a window of 6.4s.

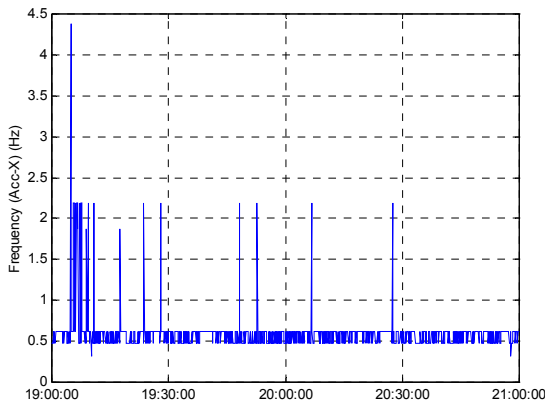


Figure 18 Time-Frequency analysis for Acc x-dir with a window of 6.4s.

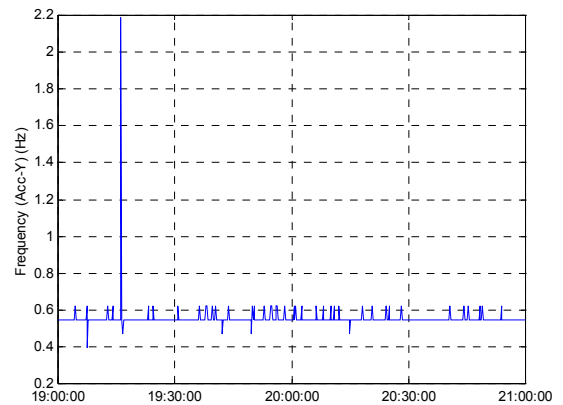


Figure 21 Time-Frequency analysis for Acc y-dir with a window of 12.8s.

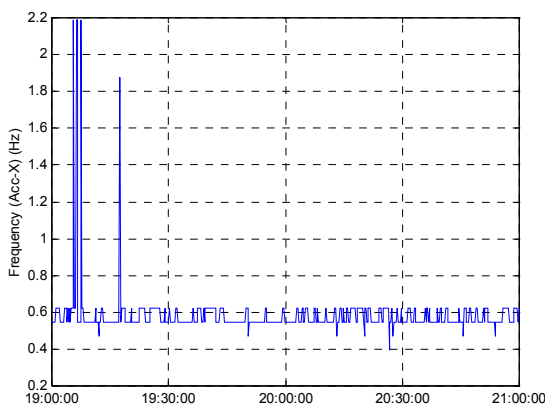


Figure 20 Time-Frequency analysis for Acc x-dir with a window of 12.8s.

All these results agree well with the previous global FFT analysis, but with the timing of events/signals, which enables cross-correlation with wind speed and direction data.

It can be seen that in general GPS can pick up signals at the low frequency end (0-0.2Hz), probably contaminated by GPS-specific noise such as multipath, while it is easier for the accelerometer to record high frequency signals (2Hz and above). *Therefore, the two sensors are complementary.* On the other hand, the two sensors do have some overlapping capability in the band between 0.2 – 2Hz, i.e., whatever is picked up by the accelerometer will also be picked up by the RTK-GPS. *This overlap provides redundancy within the integrated system which enables robust quality assurance (i.e., double integration and differentiation as shown in Section 2) and the overlapping band is likely to increase with the advancement of GPS receiver technology.*

Note currently the RTK-GPS data are collected using the single-base RTK approach. It is possible to enhance the RTK performance by employing network RTK, especially applicable in Japan considering the available nation-wide, very dense, and continuous GPS (CGPS) network.

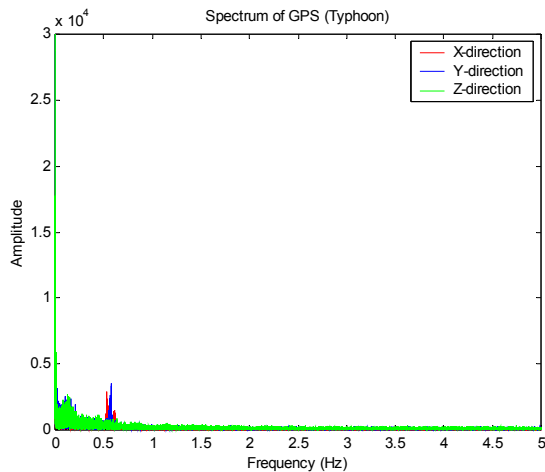


Figure 22 Overall FFT spectrums of GPS measurements during the typhoon.

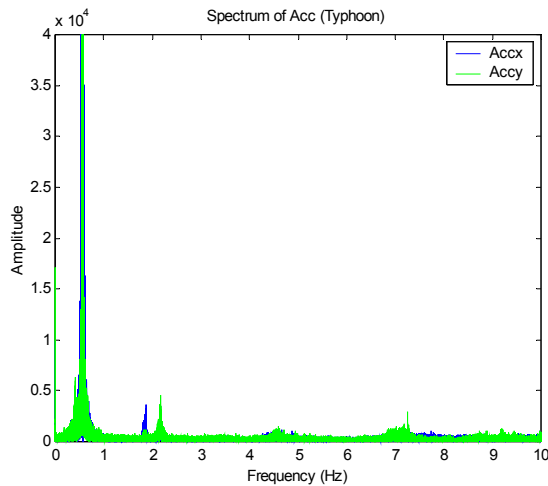


Figure 23 Overall FFT spectrums of accelerometer measurements during the typhoon.

The limitation of single-base GPS-RTK is the distance between the reference receiver and the user receiver so as to ensure that distance-dependent biases such as orbit error, and ionospheric and tropospheric signal refraction, can cancel. This has restricted the inter-receiver distance to 10km or less if very rapid ambiguity resolution is desired (i.e. less than a few seconds). Moreover, in dense urban environments the identification of a site for a reference station can be especially challenging. The reference station must have a clear view of the sky in order to track the satellites, be in close proximity to the user to minimize baseline separation errors, be relatively multipath free, and be on a stable platform. In most cases, rigid structures are low rise and often overshadowed by taller neighbouring buildings, making their ability to track satellites highly variable.

In network-RTK there is a data processing ‘engine’ with the capability to resolve the integer ambiguities between the static reference receivers that make up the CGPS

network. The ‘engine’ is capable of handling data from receivers 50-100km apart, operates in real-time, instantaneously for all satellites at elevation cut-off angles down to a couple of degrees (even with high noise data that are vulnerable to a higher multipath disturbance). The network-RTK correction messages can then be generated.

Because there will be several reference stations available in the 100km radius of the user receiver, there are several advantages of network-RTK over the standard single-base RTK configuration (Rizos, 2002):

- No need for the user to operate his own reference station (cost reduction).
- Elimination of orbit bias and ionosphere delay.
- Better reduction of troposphere delay, multipath disturbance and observation noise.
- RTK can be extended to what might be considered ‘medium-range’ baselines (up to 100km).
- Low-cost single-frequency receivers can be used for RTK (further cost reduction).
- Improve the accuracy, reliability, integrity, productivity and capacity of GPS positioning.

Therefore, network-based GPS-RTK has been proposed as a key component for the future integrated system. It will be tested on the 108m steel tower currently monitored using the single-base GPS-RTK.

4. Concluding Remarks

GPS and accelerometer sensors have been installed on a 108m tall steel tower and data have been collected at 10Hz and 20Hz during a typhoon on 1 October 2002. The wind induced deformation has been analysed in both the time and frequency domains. In the frequency domain, both the GPS and accelerometer results show strong peaks at 0.57Hz, which agrees with previous studies by using different methods, although GPS measurements are noisy in the low frequency end and accelerometer measurements at the high frequency end. Measurements have been converted to displacement (in the case of accelerometer) and acceleration (in the case of GPS) through double integration and double differentiation respectively, for the purpose of direct comparison. The results agree with each other very well, except that the static component is missing from the accelerometer derived results.

Measurements from GPS, accelerometer and anemometer have been analysed in detail using short-time FFT. The

spectrum features have been well explained using such an approach.

The benefits of an integrated system of GPS and accelerometer sensors to monitor the structural deformation have been highlighted.

Acknowledgements

The author wishes to thank several members of the Satellite Navigation And Positioning Group (SNAP) and the Photonics and Optical Communications Group (POCG) at UNSW for useful discussions and help.

Special thanks to the UNSW Faculty of Engineering for the scholarship supporting the author's PhD studies under the joint supervision of the Schools of Surveying and Spatial Information Systems, and Electrical Engineering and Telecommunications. This work would not have been possible without this joint supervision. The research is also sponsored by a Faculty Research Grant of the UNSW.

The collaboration of Professor Yukio Tamura and Mr Akihito Yoshida from the Tokyo Polytechnic University has been invaluable for these studies.

The author has benefited enormously from Associate Professor Ambikairajah's course on Digital signal processing.

Reference

Ambikairajah, E., 2003. *Digital signal processing Lecture notes*. School of Electrical Engineering & Telecommunications, the University of New South Wales, Australia.

Ashkenazi, V., & Roberts, G.W., 1997. *Experimental monitoring of the Humber Bridge using GPS*, *Proc. of Institution of Civil Engineers*, 120, 177-182.

Brownjohn, J., Pan, T.C., Mita, A., & Chow, K.F., 1998. *Dynamic and static response of Republic Plaza*, *Journal of the Institution of Engineers Singapore*, 38(2) 35-41.

Kilpatrick, J., Kijewski, T., Williams, T., Kwon, D.K., Young, B., Abdelrazaq, A., Galsworthy, J., Morrish, D., Isyumov, N., & Kareem, A., 2003. *Full scale validation of the predicted response of tall buildings: preliminary results of the Chicago monitoring project*, *Proc. 11th Intern. Conf. on Wind Engineering*, June 2-5, Lubbock, Texas, USA.

Parkinson, B., & Spilker, J., 1996. *Global Positioning System: Theory and Applications*, Washington, DC: American Institute of Aeronautics & Astronautics, 793pp.

Penman, A., Saxena, K., & Sharma, V., 1999. *Instrumentation, Monitoring and Surveillance: Embankment Dams*, A.A. Balkema: Rotterdam, 288pp.

Rizos, C., 2002. *Network RTK research and implementation: A geodetic perspective*, *Journal of Global Positioning Systems*, 1(2), 144-150.

Tamura, Y., Matsui, M., Pagnini, L.-C., Ishibashi, R., & Yoshida, A., 2002. *Measurement of wind-induced response of buildings using RTK-GPS*, *J. Wind Eng. and Industrial Aerodynamics*, 90, 1783-1793.

Tamura, Y., 2003. *Design issues for tall buildings from acceleration to damping*. 11th International Conference on Wind Engineering, June 2-5, Lubbock, Texas, USA.

Trimble, 2003. <http://www.trimble.com/ms860.html>

Yoshida, A., Tamura, Y., Matsui, M., & Ishibashi, S., 2003. *Integrity monitoring of buildings by hybrid use of RTK-GPS and FEM analysis*, 1st International Conference on Structural Health Monitoring and Intelligent Infrastructure, November 13-15, Tokyo, Japan.